

Re-examining the Lyman Continuum in Starburst Galaxies Observed with the Hopkins Ultraviolet Telescope

Mark Hurwitz, Patrick Jelinsky, and W. Van Dyke Dixon
Space Sciences Laboratory, University of California,
Berkeley, CA 94720-7450

ABSTRACT

We have reevaluated the constraints on the Lyman continuum emission from four starburst galaxies observed with the Hopkins Ultraviolet Telescope (HUT) during the Astro-2 mission. Applying a detailed model of the absorption by interstellar gases in our Galaxy, and using the latest HUT data products, we find upper limits to the redshifted Lyman continuum that are less restrictive than those reported previously (Leitherer et al. 1995 ApJ, 454, L19). Well determined astrophysical and instrumental effects permit 2σ upper limits no tighter than 5.2%, 11%, 57%, and 3.2% to be set on the escape fraction of Lyman continuum photons from IRAS 08339+6517, Mrk 1267, Mrk 66, and Mrk 496, respectively. Absorption from undetected interstellar components (including H₂) or modulation of the emergent spectrum by gas or dust in the parent galaxy could allow the true escape fractions to exceed these revised upper limits.

1. INTRODUCTION

In a recent study, Leitherer et al. (1995) set upper limits on the fraction of Lyman continuum photons escaping from four starburst galaxies observed with the Hopkins Ultraviolet Telescope (HUT). The 2σ upper limit, expressed as a fraction of the number of ionizing photons produced (estimated from Balmer emission line strengths), was typically found to be about 3%. Star-forming regions in galaxies of this type are generally heavily reddened; the escape of Lyman continuum photons thus depends sensitively on the patchiness of the absorbers in the star-forming galaxy. Because the patchiness is difficult to constrain independently, the study of Leitherer et al. is important despite the small sample size.

The emergent Lyman continuum flux can be constrained experimentally by setting limits on the observed source brightness between 915 Å and the redshifted Lyman limit of the galaxy under study (which falls between 929 and 939 Å for this sample). Leitherer et al. assume that the intrinsic spectrum is flat in this region and that Galactic absorption, other than extinction by dust, can be neglected. In this work we address the last assumption in some detail and demonstrate that Galactic gas-phase absorption attenuates a significant fraction of the flux between 915 Å and the redshifted Lyman limit along these sight lines, leading to looser constraints on the fraction of ionizing photons that may escape the starburst galaxy.

2. MODELING THE GALACTIC ABSORPTION

The basis for our absorption models is the Bell Labs 21 cm survey (Stark et al. 1992), which maps N_{HI} , the primary gas phase absorber at the wavelengths of interest, in 10 km s^{-1} velocity channels. For each sight line we adopt the 21 cm profile from the nearest beam of the survey; these profiles are shown in Figure 1. To approximate the smooth distribution of H I with velocity, we assign a Doppler b value of 4.3 km s^{-1} to a numerical “cloud” centered at each velocity channel. We adopt a profile for O I identical to that of H I, but with a column that is lower by 3.3 dex (de Boer 1981).

In physical clouds, the b values of the heavier elements may well be lower than that of H I. However, the broad range of velocities at which H I is observed must be dominated by bulk motions or turbulence rather than thermal widths. The O I contributes only about 7% of the total equivalent width of the gas phase absorption, so even fairly gross errors in its velocity distribution would have a small effect on our final results. Other atomic species with absorption features in the bandpass of interest include N II, N* II, Ar II, Fe II, Al II, and S VI; we neglect these on the grounds that their contribution to the absorption will be fairly low and/or that their column is difficult to predict.

To calculate the far ultraviolet absorption expected from a given 21 cm profile, we establish a very fine wavelength grid (0.001 \AA) and calculate exact Voigt profiles for the species and velocity components along the sight line. We co-add the optical depths, exponentiate, and convolve with a 3 \AA FWHM Gaussian to approximate the HUT resolution. (Small differences between our assumed resolution and the actual value will have no effect on the end result.) We then bin the transmission on a 0.51 \AA grid to match the HUT detector pixels. We show a sample interstellar absorption profile, calculated for IRAS 08339+6517, in Figure 2.

To assess the statistical uncertainty in the far ultraviolet gas phase absorption, we vary the H I column in each velocity channel in Monte Carlo fashion, assuming a Gaussian distribution centered on the measured value but with a 1σ uncertainty of 10^{17} cm^{-2} in each channel. This uncertainty is typical of the empirical excursions in the wings of the 21 cm line, which extend out to $\pm 360 \text{ km s}^{-1}$. The true probability of encountering a 10^{17} cm^{-2} cloud at a given velocity is not easy to predict, but, at least at the velocity extrema, it is presumably lower than would be estimated from the measurement error. We therefore crop the profile beyond 30 km s^{-1} from the velocity range within which H I is clearly detected. The resulting interstellar transmissions and statistical uncertainties are shown in Table 1.

3. DATA REDUCTION AND ANALYSIS

The observations of starburst galaxies were performed with HUT on the Astro-2 mission of the space shuttle *Endeavour* in 1995 March. HUT is a far-UV spectrophotometer with first-order

Table 1. Summary of analysis of the four starburst galaxies observed with HUT.

Galaxy	Integ ^a	Src ^b	Err ^c	BG ^d	Err ^e	Net ^f	Err ^f	Band ^b	T_{ism}^g	Err	Flux ^h	F_{esc}^i
(1)	(s)	(3)	(4)	(counts)		(7)	(8)	(Å)	(10)	(11)	(12)	(%)
(1)	(2)	(3)	(4)	(5)	(6)	(7)	(8)	(9)	(10)	(11)	(12)	(13)
IRAS 08339 +6517	2752	41	6.4	43.3	3.4	-2.3	7.3	13.8	0.44	0.014	< 1.7	< 4.1
Mrk 1267	3062	37	6.1	34.9	3.2	2.1	6.9	14.3	0.56	0.013	< 1.4	< 8.5
Mrk 66	2176	40	6.3	41.4	3.7	-1.4	7.3	16.8	0.49	0.017	< 1.6	< 43
Mrk 496	1410	51	7.1	52.1	4.9	-1.1	8.7	23.5	0.63	0.014	< 1.6	< 2.3

^aEffective integration time in seconds.

^bRaw detector counts from 915 Å to the redshifted Lyman limit; the width of the band is shown in column 9.

^cSquare root of column 3.

^dBackground expected in this wavelength interval, scaled from raw counts in the 850 – 900 Å region.

^eStatistical error in column 5.

^fNet counts and statistical error therein.

^gMean interstellar transmission within the band, including only the known atomic species.

^hThe 2σ maximum permitted flux at Earth, corrected for gas phase absorption (but not for extinction, for ease of comparison with Leitherer et al. 1995). Units are $\times 10^{-15}$ erg (cm² s Å)⁻¹.

ⁱCorresponding limit on the escape fraction for ionizing photons from the galaxy, scaled from Leitherer et al. Note that the limits in columns 12 and 13 may be unrealistically low for reasons discussed in the text.

sensitivity extending from 820 to 1840 Å at 0.51 Å pixel⁻¹; its resolution ranges from 2.1 to 2.5 Å FWHM between 900 and 950 Å. The spectrograph and telescope are described in detail by Davidsen et al. (1992), while Kruk et al. (1995) discuss its performance and calibration on the Astro-2 mission.

Four starburst galaxies, IRAS 08339+6517, Mrk 1267, Mrk 66, and Mrk 496 (= NGC 6090), were observed several times during the Astro-2 mission. Basic parameters of the galaxies and their flux-calibrated HUT spectra may be found in Leitherer et al. (1995). For each observation, data products from the HUT “Ballistic Process” data-reduction system have been kindly provided by G. Kriss. We exclude from our analysis observations in which the source appears to spend more than 50% of the observation outside of the aperture, based on plots of source count rate vs. time. All the observations included here were taken through the 20'' circular aperture. Spectra from multiple observations were co-added; total integration times are listed in Table 1. For Mrk 496, we have scaled the integration time by 0.8 to account for excursions of the target from the aperture, bringing the HUT flux at longer wavelengths into agreement with the *IUE* measurements of Kinney et al. (1993).

We carry out most of our analysis of the spectra using raw counts rather than calibrated flux units, because detector dark counts and stray light (which dominate the signal below the redshifted Lyman limit) are expected to be “flatter” in raw counts. We sum the source counts from 915.0 Å to the redshifted Lyman limit, adopting the radial velocities from Leitherer et al. We estimate the background in this interval by scaling the summed counts from 850 to 900 Å.

Treating both the background-subtracted source counts and the mean interstellar transmission as independent Gaussian variables with σ shown in Table 1, we can arrive at a 95% upper limit on the photon flux incident on the Galaxy (but not yet corrected for Galactic dust extinction), which we then multiply by the photon energy, and divide by the product of the integration time, effective area, and bandpass in Å. The results are summarized in Table 1, where the final column (escape fraction) is scaled from Leitherer et al., assuming the Galactic extinction and H α luminosity for each galaxy from the previous work.

To explore the sensitivity of our results to the detailed choice of statistical technique, we have applied two alternative methods. The first is an analysis similar to the one described above, except we first exclude those wavelength bins for which the mean gas-phase interstellar transmission is less than 0.5 (from 915 to, typically, 920 Å). This reduces the effective bandpass of the exposure, but raises the mean interstellar transmission over the remaining interval. In all cases, the final result is within 12% of the value cited in Table 1. We have also applied a maximum likelihood method. Here the alternative statistical treatment sometimes yields a more significant difference; the largest is for Mrk 1267, where the flux constraint is 75% of the value in Table 1.

4. OTHER SOURCES OF UNCERTAINTY

We now consider whether effects other than the shot noise in the detector counts could affect our limits on the Lyman continuum escape fraction.

Our estimate of the per-pixel background, comprising detector dark counts and stray light, is insensitive to the detailed endpoints of the adopted extreme ultraviolet wavelength interval. The background in the 840 – 885 Å band is consistent, within fairly small statistical uncertainties, with that in the 850 – 900 Å band, indicating that our background estimate is not affected by bright airglow features near the endpoints.

To explore the potential variation of the background with wavelength, we analyzed ten HUT spectra for which the source was either negligibly faint or outside the aperture completely. In four of four blank sky spectra collected through the $19'' \times 197''$ aperture, and in five of six spectra collected through the $10'' \times 56''$ aperture, the background is higher at 920 Å than in the extreme ultraviolet. The relative contributions of stray light and detector dark count rate can be estimated from the variation in the total background flux with aperture area. Extrapolating to the 20'' diameter aperture used in this work, we find that the detector dark counts, not the stray light, contribute the vast majority (circa 80%) of the background near 920 Å in these spectra.

The reliability of the background subtraction therefore depends primarily on the flatness of the detector dark counts spectrum. Greeley (1995, private communication) has compiled nearly 11 on-orbit hours of dark counts data, which we have searched for nonuniformities. At phosphor voltage level 3, the dark spectrum between 915 and 930 Å is marginally (2%) higher than the level between 850 and 900 Å with a 1σ uncertainty corresponding to 8% of the mean level. At phosphor voltage level 4, there is evidence for a genuine variation. At this voltage the count dark spectrum between 915 and 930 Å is 13% lower than the level between 850 and 900 Å with a 1σ uncertainty corresponding to 5.5% of the mean level. More than half of the observations of IRAS 08339+6517, and all of the observations of the remaining three starbursts, were collected at phosphor voltage level 4. Although this effect would not be credible in the absence of independent data, columns 7 and 8 of Table 1 provide some evidence for an oversubtraction of the background flux.

We reanalyze the starburst spectra, correcting for a 13% of background systematic subtraction offset and a 5.5% of background statistical uncertainty (added in quadrature with the shot noise). Inclusion of these effects raises the 95% upper limit on the escape fractions to 5.2%, 11%, 57%, and 3.2% for IRAS 08339+6517, Mrk 1267, Mrk 66, and Mrk 496, respectively.

A second effect is the potential for additional gas phase absorption from the interstellar medium. Our assessment of the statistical uncertainties in the absorption is an oversimplified treatment, given the complexities of the 21 cm baseline subtraction, calibration, etc. *The radio surveys cannot rule out the existence of clouds whose convergent Lyman series would add significant attenuation to the absorption curves found here.* Independent constraints on such

clouds would require high resolution, high signal-to-noise far-ultraviolet spectra, which will be challenging given the faintness of the sources. For two of the galaxies (IRAS 08339 and Mrk 1267), the known H I column is sufficiently high that significant H₂ is likely to be present (Savage et al. 1977), and for the other two galaxies, its presence cannot be ruled out. The quantitative effect of additional H I or H₂ clouds on the transmission of the interstellar gas depends on many parameters, all of them difficult to constrain independently. The authors’ subjective assessment is that it would be prudent to revise the previously listed upper limits upward by a factor of about 1.25 to account for additional interstellar components. Even more substantial revisions may be necessary if the clouds are present over a wide velocity range.

Finally, we must remain cognizant of the potential for interstellar absorption in the *parent* galaxies. Leitherer et al. demonstrate that the production of ionizing photons immediately below the Lyman limit is well correlated with the production of ionizing photons of all wavelengths for a broad range of stellar mass distributions. Photoelectric absorption by H I in the parent galaxy will of course attenuate the longest wavelengths most strongly. Dust grains can produce a similar effect, serving as the primary cause of extinction immediately below the Lyman limit if the escape paths are filled with highly ionized hydrogen (e.g., less than about 4×10^{-4} neutral) with a standard gas-to-dust ratio. Below the Lyman limit, interstellar grains tend to absorb rather than scatter. As the photon wavelength decreases from 912 Å to about 90 Å, the dust cross section falls by a factor of about 3 (Martin & Rouleau 1991). Like H I, dust preferentially absorbs photons immediately below the Lyman limit, opening the possibility that the escape fraction for higher energy photons could be significantly greater than the values derived from observations of galaxies at these comparatively low velocities.

5. DISCUSSION AND CONCLUSIONS

We have shown that astrophysical and instrumental effects permit 2σ upper limits no tighter than 5.2%, 11%, 57%, and 3.2% to be set on the escape fraction of Lyman continuum photons from IRAS 08339+6517, Mrk 1267, Mrk 66, and Mrk 496, respectively. Additional interstellar absorption would permit the true escape fraction to be higher than these limits. The effect of such absorption is difficult to quantify but a subjective assessment indicates that a multiplicative factor of 1.25 would be prudent. Differential absorption across the Lyman continuum by interstellar material in the parent galaxy would permit the true escape fraction to be higher still.

Madau & Shull (1996) estimate, based on the metal enrichment of Ly α clouds, that massive stars could contribute significantly to the UV background at early epochs if about 25% or more of the Lyman continuum photons can escape the star-forming regions. Our revised upper limits are significantly closer to this escape fraction than were those reported previously. We have, thus, measurably reduced the weight of evidence—albeit preliminarily—against the hypothesis that Lyman continuum photons from massive stars contribute to the ionization of the universe at early epochs.

The complex absorption caused by the gas phase of the ISM near the Galactic Lyman limit, and the difficult-to-characterize uncertainties therein, can be largely sidestepped by observing starburst galaxies at higher velocity. To be conservative, the region shortward of about 930–940 Å in the observer’s frame (depending on resolution) should be considered suspect. Target galaxies with redshifts greater than about 12,600 km s⁻¹ would be highly desirable, although the potential for interstellar absorption in the parent galaxy will remain a difficulty even at these velocities.

We would like to thank G. Kriss for providing output products from the HUT Ballistic Process data-reduction system. The Hopkins Ultraviolet Telescope Project is supported by NASA contract NAS5-27000 to Johns Hopkins University. We acknowledge the support of NASA grant NAG5-696, and the helpful comments of the anonymous referee.

REFERENCES

- de Boer, K. S. 1981, *ApJ*, 244, 848
- Davidson, A. F., et al. 1992, *ApJ*, 392, 264
- Kinney, A. L., Bohlin, R. C., Calzetti, D., Panagia, N., & Wyse, R. F. G. 1993, *ApJS*, 86, 5
- Kruk, J. W., Durrance, S. T., Kriss, G. A., Davidson, A. F., Blair, W. P., Espey, B. R., & Finley, D. 1995, *ApJ*, 454, L1
- Leitherer, C., Ferguson, H. C., Heckman, T. M., & Lowenthal, J. D. 1995, *ApJ*, 454, L19
- Madau, P. & Shull, J. M. 1996, *ApJ*, 457, 551
- Martin, P. G. & Roleau, F. 1991, in *Extreme Ultraviolet Astronomy*, ed. R. F. Malina & S. Bowyer (New York: Pergamon), 341
- Savage, B. D., Bohlin, R. C., Drake, J. F., & Budich, W. 1977, *ApJ*, 216, 291
- Stark, A., Gammie, C., Wilson, R., Bally, J., Linke, R., Heiles, C., & Hurwitz, M. 1992, *ApJS*, 79, 77

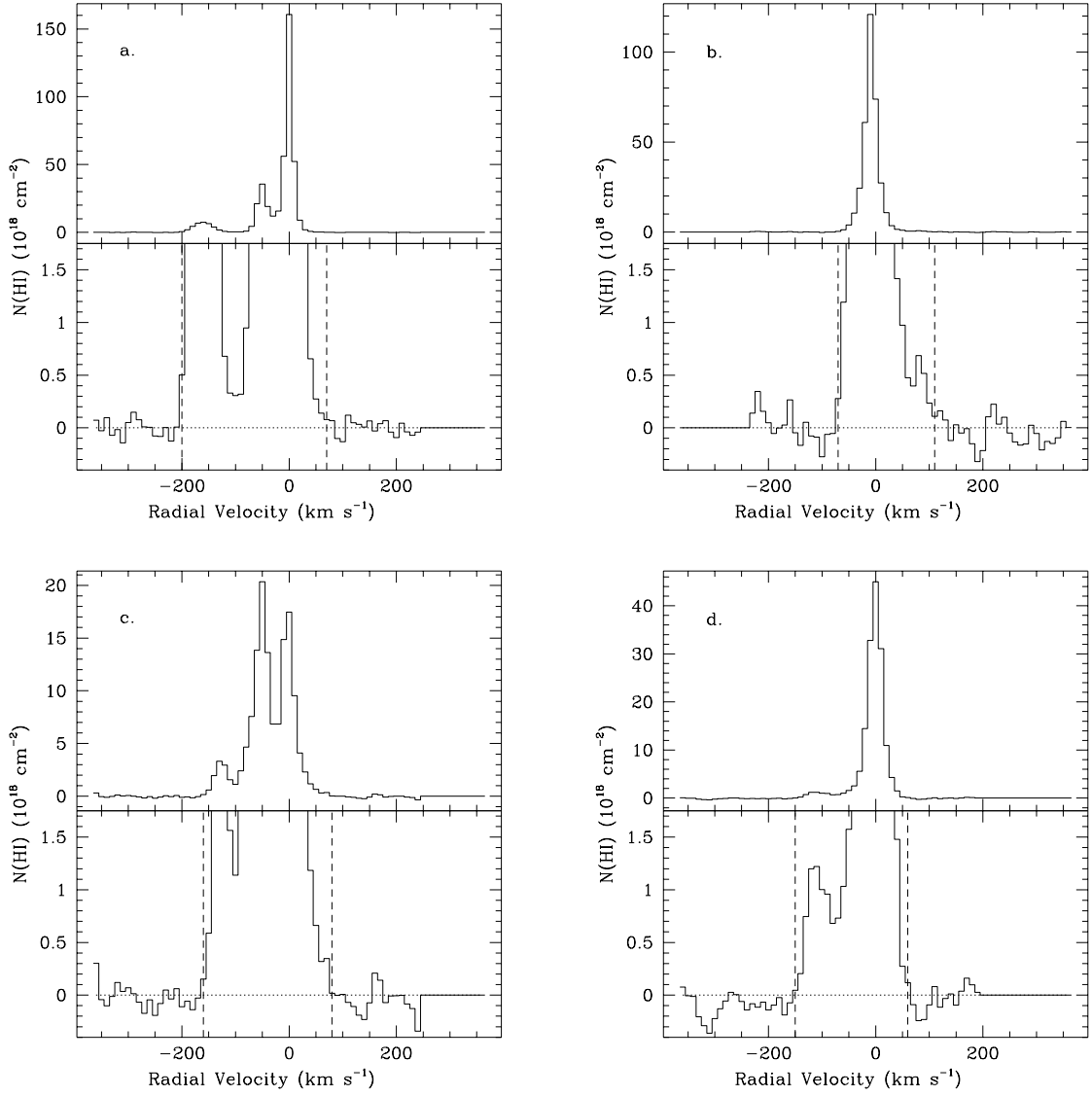


Fig. 1.— HI 21 cm profiles from Stark et al. for the four starburst sight lines of (a) IRAS 08339+6517, (b) Mrk 1267, (c) Mrk 66, and (d) Mrk 496. Vertical dashed lines indicate the velocity range within which we assume that the HI detections are secure.

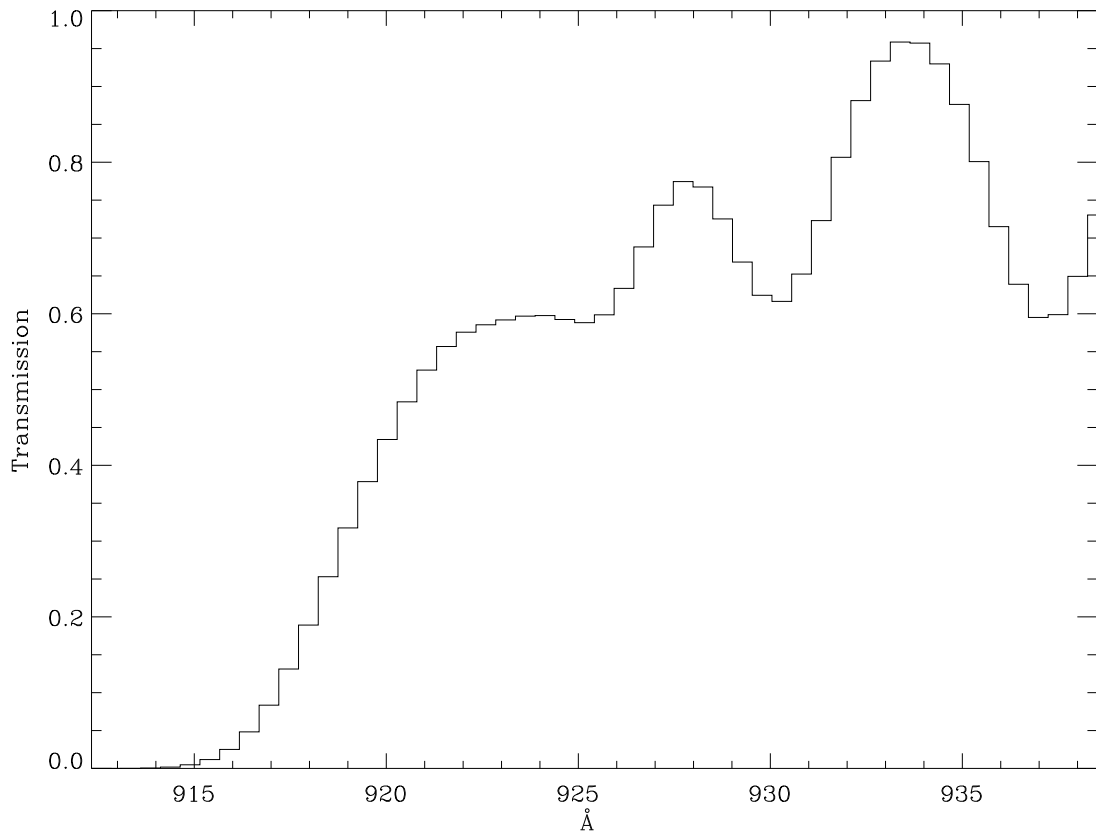


Fig. 2.— Gas phase interstellar medium transmission curve calculated for the sight line toward IRAS 08339+6517. Theoretical transmission has been convolved with a 3 \AA FWHM Gaussian and rebinned at 0.51 \AA . Only H I and associated metal lines are included.